33B.0 IN-SITU STUDIES OF STRAIN RATE EFFECTS ON PHASE TRANSFORMATIONS AND MICROSTRUCTURAL EVOLUTION IN MULTI-PRINCIPAL ELEMENT ALLOYS

John Copley (Mines)
Faculty: Amy Clarke (Mines)
Other Participants: Francisco Coury (UFSCar)
Industrial Mentor: Clarissa Yablinsky (LANL), Paul Wilson (Boeing), John Foltz (ATI)

This project initiated in Fall 2018 and is supported by the Office of Naval Research. The research performed during this project will serve as the basis for a MS thesis program for John Copley.

33B.1 Project Overview and Industrial Relevance

Multiple Principle Element Alloys (MPEAs) have gained recent interest, as they represent a relatively unexplored alloy design space, being centered in, rather than at the corners, of ternary, quaternary and quinary phase diagrams [33B.1]. Some MPEAs, especially those from the CoCrNi family, have the potential to exhibit TRansformation and TWinning induced plasticity (TRIP and TWIP respectively), where plastic deformation is accommodated by shifts in the stacking sequence of specific atomic planes, in addition to dislocation motion [33B.2]. The combination of TRIP/TWIP, in addition to dislocation motion and multiplication, results in high work hardening rates, as the boundaries of transformation product and twin interfaces act as barriers to dislocation motion [33B.3]. Materials with high work hardening rates are, in turn, associated with increased ductility and strength when compared to materials with otherwise similar properties and lower work hardening rates, as predicted by the Considère instability criterion $\sigma = d\sigma/d\varepsilon$. The influence of strain hardening rate on ultimate tensile strength and uniform elongation in a tensile test is illustrated in **Figure 33B.1.** Increasing the ductility of a material without a corresponding decrease in strength increases the area under the stress-strain curve. A larger area under a stress strain curve indicates a larger specific plastic work to fracture, which is one measure of toughness.

Materials with high toughness are useful in engineering applications, as they are able to absorb higher amounts of energy before failure. High energy absorption is especially useful for blast resistance, which is the primary focus of this project. Increased energy absorption/toughness reduces the required amount of armor for similar protection against explosive reactions. Outside of blast resistance, the extended ductility of TRIP/TWIP materials improves their formability, allowing them to be worked into complex geometries that require higher strains. Studies of the effects of strain rate and state, as well as phase stability and deformation mechanisms, on the deformation behavior and microstructural evolution of MPEAs will enable alloy design for specific applications. Furthermore, better fundamental understanding of TRIP/TWIP behavior may have extensions to more commonly used advanced high strength steels that exhibit TRIP/TWIP behavior, in addition to metastable β-titanium alloys – a complementary project underway in CANFSA.

33B.2 Previous Work

33B.2.1 Literature Review

A review of the existing literature reveals a few families of MPEAs that have received much attention. The Cantor Alloy, an equi-atomic CoCrFeMnNi FCC solid solution, has been shown to be the toughest true high-entropy-alloy (with an entropy of mixing greater than 1.5R) [33B.1]. Work by George *et al*. has shown that the equi-atomic CoCrNi medium entropy alloy has superior strength and ductility as compared to the Cantor alloy [33B.4]. Work on CoCrNi equi-atomic alloys has shown the formation of nano-twins during deformation resulting in enhanced strength and toughness at cryogenic temperatures when twinning becomes more prominent [33B.5]. As compared to other material systems, CoCrNi alloys have promising combinations of strength and ductility. Accordingly, the CoCrNi ternary system was selected as the initial system of interest in this work. Work performed by Coury *et al*. using a solid solution strengthening model designed for HEAs (called EARS or Effective Atomic Radii for Strengthening) showed that superior properties could be found using non-equiatomic compositions, and there is significant room for optimization over the Cantor alloy [33B.6]

33B.2.2 Initial Investigation of TRIP in $Co_{55}Cr_{40}Ni_5$

Evidence of TRIP behavior in an FCC $Co_{55}Cr_{40}Ni_5$ MPEA was seen following cold rolling to 25% by Dr. Francisco Coury during his PhD work. Initial microstructural characterization of the cold rolled material showed the presence of both deformation twins and an HCP transformation product. Thermo-Calc modeling of T_o, the temperature at which the two phases have the same free energy and the same composition, indicated a high T_o (approx. 1000 °C) for this alloy. A 2 kg ingot of the $Co_{55}Cr_{40}Ni_5$ alloy was prepared via spray-forming at the Federal University of Sao Carlos (UFSCar), in Brazil by Dr. Guilherme Zepon. This ingot was used for *in-situ* synchrotron X-ray diffraction (XRD)/thermo-mechanical experiments conducted at the Brazilian Light Source (LNLS). The XRD/thermo-mechanical tests were performed using quasi-static strain rates at a variety of temperatures, ranging from -100 °C to 900 °C. The XRD data show transformation of the FCC phase to HCP during deformation in all tests conducted from -100 °C to 450 °C. Data showing the appearance of an HCP phase in the XRD data with increasing strain is included as **Figure 33B.2**. For temperatures above 450 °C, the XRD data does not show evidence of the HCP phase, indicating the deformation-induced transformation is suppressed.

33B.2.3 Initial High Rate Experiments at the APS in Early 2019

This project, as well as its compliment focusing on metastable β-titanium alloys (Project #33A), were awarded beam time from a general user proposal at the Advanced Photon Source (APS) at Argonne National Laboratory. *In-situ* XRD and Kolsky bar (Split-Hopkinson bar) compression and tension experiments were conducted at the APS 32-ID-B beamline, with the goal of observing phase evolution due to TRIP behavior at high strain rates (on the order of 10^3 s^{-1}) and dynamic response during deformation. Four alloys were selected using Thermo-Calc modelling of the diffusionless transformation temperature ($Co_XCr_{40}Ni_{60-X}$ where X=55, 50, 40, and 30 at. %, hereafter referred to by their cobalt content Co30, Co40, etc.) and the equi-atomic CoCrNi, were produced by arc melting. These alloys were selected to have a wide range of T_o and be within the single phase FCC region at 1100 °C. Analysis of the XRD data shows the evolution of a few individual spots to diffuse rings upon deformation, indicating crystallite refinement possibly from the formation of deformation twins, as illustrated in **Figure 33B.3**. Use of HiSPoD, or High-Speed Polychromatic Diffraction, a MATLAB program built to analyze data collected during high speed *in-situ* experiments at Sector 32-ID at the APS allowed for rapid processing of the collected *in-situ* XRD data [33B.7]. In the CoCrNi samples, high absorbance by the material resulted in relatively low diffracted intensities and complications due to the polychromatic nature of the "pink" beam at the APS.

33B.3 Recent Progress

Recent experiments in February of 2020 at sector 32 of the APS using samples 100 μm and 200 μm in thickness showed significantly improved diffraction data as compared to initial experiments of early 2019. This is attributed to the use of thinner samples and the use of a better detector (sample thickness effects are discussed in this project's Fall 2019 report in section **33B.3.1**). As with the experiments from February 2019, five alloys were prepared via arc melting. The buttons produced by arc melting were then forged into small rectangular prisms in an effort to produce a geometry more suitable to machining as well as to reduce the grain size without introducing significant texture. These alloys are commonly cold rolled and recrystallized to produce a fine-grained microstructure, but this can result in significant texture. The resulting grain size was on the order of 80-100 μm. As such, significant variation in the mechanical data collected, especially from the 100 μm thick samples is possible. However, the lack of texture and ability to machine the large numbers of samples made this an attractive option, despite the relatively large grain sizes.

Of the five alloys selected for testing, two were believed to be TWIP alloys. These two alloys, the equiatomic CoCrNi and the Co30 alloy, were predicted by Thermo-Calc to be unable to experience TRIP type behavior due to a T_0 of 0 K. Effectively, these alloys do not have HCP as a stable phase, and so the distance between the FCC and HCP free-energy vs composition curves is large, and they do not intersect at any finite temperature. The other three alloys tested, Co40, Co50, and Co55, have T_0 temperatures in the range of 400-1000 °C, where increasing Co content corresponds to increasing T_0. These alloys have been shown to experience TRIP behavior during cold rolling while preparing samples, and the Co55 has been shown to transform during *in-situ* deformation with XRD at the Brazilian light source. Of these alloys, the Co50 and Co55 exhibited transformation during high rate deformation at the APS, as illustrated in **Figure 33B.4**. For both of these alloys, initial diffraction patterns are spotty then evolve to full rings followed by the evolution of a new peak between the FCC {111} and {200} peaks. This new peak is believed to be an HCP $\{10\bar{1}1\}$

peak. The TWIP alloys did not exhibit this new peak, but did show evolution from initially spotty patterns to full rings. While this is not conclusive evidence of deformation twinning, it is the most probable explanation in these alloys that have low stacking fault energies, especially at higher deformation rates, where the formation of dislocation structures could enable more grain rotation, are suppressed [33B.8]. Co40, with the lowest diffusionless transformation temperature (407 °C), did not show evidence of transformation, with diffraction patterns behaving identically to those of the Co30 and CoCrNi alloys. The suppression of TRIP could be a result of the thermodynamic requirements for TRIP as well as the kinetic effects of strain rate on the relative favorability of different deformation mechanisms. The T_0 temperature of Co40 may have been low enough for adiabatic heating to have resulted in a sample temperature high enough to suppress the transformation. In the Co55 alloy, transformation was suppressed during quasi-static deformation between 450 °C and 600 °C, roughly 50-70 % of T_0. The corresponding range of diffusionless transformation temperatures (50-70 % of T_0) for Co40 is 70 - 200 °C which may have been reached during testing at strains rate of $\approx 10^3 s^{-1}$. Additionally, twinning as a deformation mechanism is favored at higher strain rates [33B.8], and the lowered favorability of transformation indicated by operating at a higher fraction of T_0 may have made twinning more favorable. Additional testing at elevated temperatures may elucidate the causes for the suppression of TRIP.

33B.4 Plans for Next Reporting Period

Recent data collected at the APS shows strong evidence of TRIP behavior in two Co-rich MPEAs. Further analysis of the data and samples will require post mortem diffraction, including laboratory XRD on the deformed gauge sections to determine with greater accuracy the transformed fractions as well as electron back-scatter diffraction (EBSD) on selected samples to investigate the transformed fractions and potential morphology of the transformation product. Additionally, analysis of the mechanical data as well as correlation between the mechanical data and diffraction/imaging data will need to be performed.

This project and its complement studying β-Ti alloys was awarded beam time at the Cornell High Energy Synchrotron Source (CHESS) to perform quasi-static deformation experiments with XRD at temperatures up to 300 °C. The initially scheduled beam time for these experiments in March 2020 was cancelled due to concern over COVID-19, but should be re-allocated in the future. Dr. Darren Pagan, at CHESS, has volunteered to run a few samples to allow for initial investigation before beam time is re-allocated. The selected CoCrNi samples and testing conditions focus on identifying the effects of temperature on the suppression of TRIP by testing at various fractions of T_0 in Co40, especially between 50 – 70 %, where the Co55 TRIP behavior was suppressed in prior testing. This will require similar analysis to the data collected at the APS.

Mechanical testing of sub-sized samples will be performed at Mines. Interrupted tests and temperatures outside the range achievable during the postponed CHESS experiments will be tested to expand understanding of the temperature effects on TRIP. Additionally, strain rates between those tested at the APS ($\dot{\varepsilon} \approx 10^3\ s^{-1}$) and CHESS ($\dot{\varepsilon} \approx 10^{-3}\ s^{-1}$) may be investigated at Mines. Materials and samples are already prepared for these tests. Additional materials and samples will be produced as needed.

Kolsky-bar testing of larger samples maybe performed at Los Alamos National Laboratory to complement the high rate data collected at the APS. This should provide more representative, "bulk" mechanical testing data for high rate deformation as compared to the small-scale APS testing.

The β-Ti complement to his project has been awarded beam time at Sector 1-ID at the APS where full ring detectors will enable investigation of texture changes during straining that may elucidate the twinning behavior of these materials. The timing on this beam time has not been announced, but some samples of CoCrNi MPEAs may be tested.

33B.5 References

[33B.1] D.B. Miracle, J.D. Miller, O.N. Senkov, C. Woodward, M.D. Uchic, J. Tiley, Exploration and Development of High Entropy Alloys for Structural Applications, Entropy 16 (2014) 494-525.

[33B.2] Y. Deng, C.C. Tasan, K.G. Pradeep, H. Springer, A. Kostka, D. Raabe, Design of a twinning induced plasticity high entropy alloy, Acta Materialia 94 (2015) 124-133.

[33B.3] L. Liu, B. He, M. Huang, The Role of Transformation-Induced Plasticity in the Development of Advanced

High Strength Steels, Advanced Engineering Materials article number 1701083 (2018).

[33B.4] G. Laplanche, A. Kosta, C. Reinhart, J. Hunfeild, G. Eggeler, E.P. George, Reasons for the superior mechanical properties of medium-entropy CrCoNi compared to high-entropy CrMnFeCoNi, Acta Materialia 128 (2017) 292-303.

[33B.5] B. Gludovatz, A. Hohenwarter, K. Thurston, H. Bei, Z. Wu, E.P. George, R. Ritchie, Exceptional damage-tolerance of a medium-entropy alloy CrCoNi at cryogenic temperatures, Nature Communications article number 10602 (2016).

[33B.6] F. Coury, K. Clarke, C. Kiminami, M. Kaufman, A. Clarke, High throughput discovery and design of strong multicomponent metallic solid solutions, Scientific Reports. 8 (2018) Article number 8600.

[33B.7] T. Sun, K. Fezzaa, HiSPoD: a program for high speed polychromatic X-ray diffraction experiments and data analysis on polycrystalline samples, Journal of Synchrotron Radiation, Vol. 23(4) (2016) 1046-1053.

[33B.8] G.T. Gray, High-Strain-Rate Deformation: Mechanical Behavior and Deformation Substructures Induced, Annual Review of Materials Research, Vol. 42 (2012) 285-303

33B.6 Figures and Tables

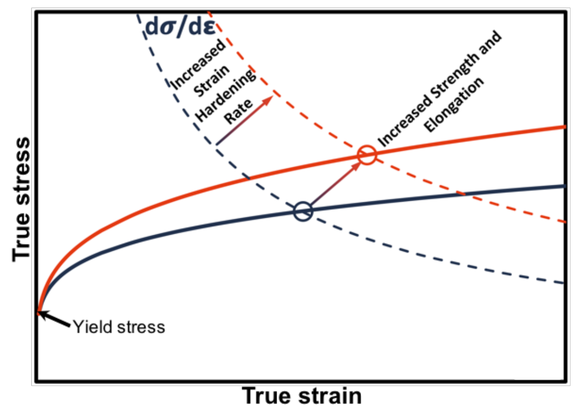

Figure 33B.1: Schematic stress strain curves for two materials with similar properties (elastic modulus, yield strength), but with different work hardening rates. Predicting the onset of necking by the instability criterion, σ=dσ/dε, shows an increase in both ultimate tensile strength and uniform elongation associated with an increase in work hardening rate.

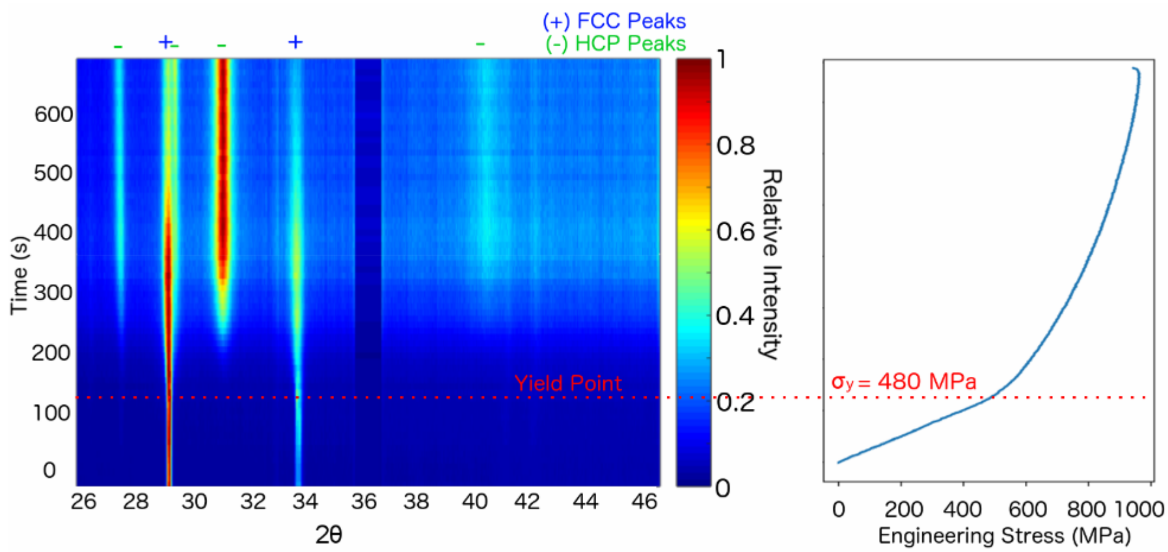

Figure 33B.2: XRD and stress-strain data for the Co0.55Cr0.40Ni0.05 alloy tested at 60 °C, showing the evolution of HCP phase at the expense of the FCC phase. The transformation begins almost immediately post yield (the temporal resolution of the XRD is insufficient to determine if some small strains exist before transformation). Testing performed by Dr. Francisco Coury at the Brazilian Synchrotron Light Laboratory (LNLS) using X-rays with wavelength of 1.033Å. Peaks associated with the HCP phase are marked with a green (-) and those associated with the FCC phase are marked with a blue (+).

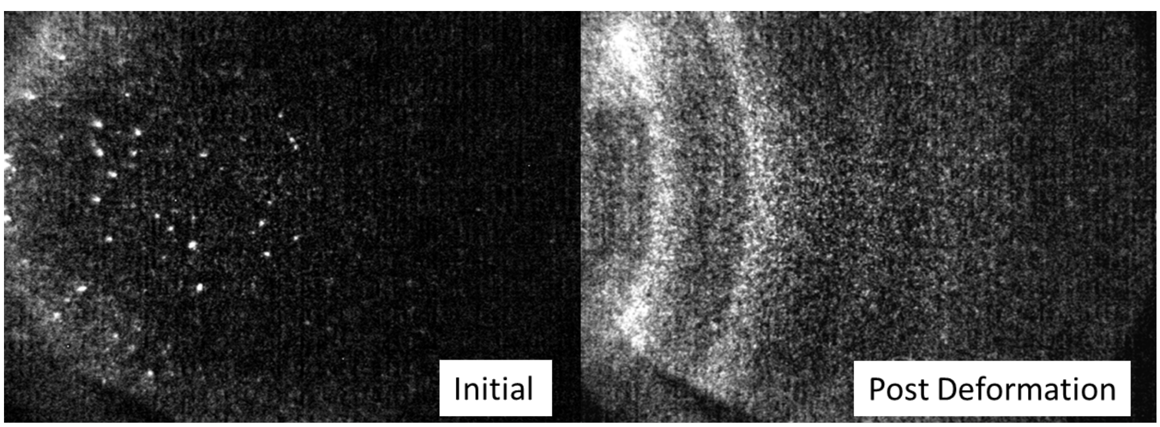

Figure 33B.3: Early diffraction patterns collected for a Co40 compression cylinder before and after deformation, showing the evolution of full diffraction rings from originally spotty patterns. This is indicative of domain refinement, and in alloys known to experience significant deformation twinning, is suggestive of TWIP behavior. The first ring of high intensity, near to the left side of the righthand image, is associated with the 2nd harmonic (a higher energy component of the incident beam).

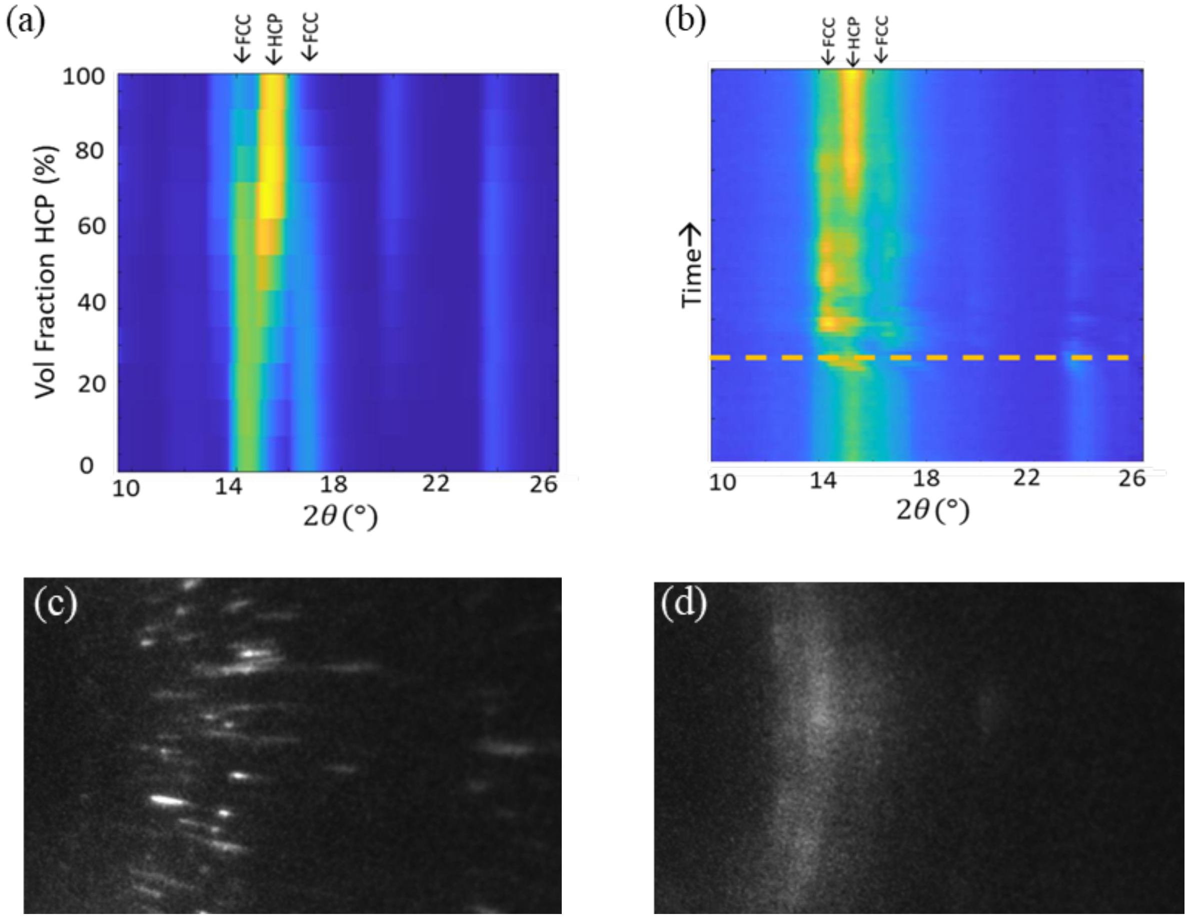

Figure 33B.4: Comparison of simulated integrated X-ray diffraction patterns (incident beam $\lambda = 0.51$ Å) showing complete transformation from FCC to HCP phase (a) with collected integrated diffraction patterns for the $Co_{55}Cr_{40}Ni_5$ alloy (b) unintegrated patterns showing the evolution from spotty points (c) to full rings (d) during high rate deformation ($\dot{\varepsilon} \approx 10^3\ s^{-1}$). In (b) the onset of straining is marked with a dashed orange line.